Medicine & Clinical Science

Original Article

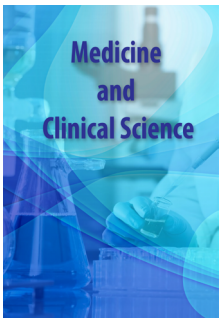

Computational Nanomaterials Design: Towards The Realization of Nanoparticle Use in Radiotherapy - Case Study 1: Adsorption States of I on Au(111) Surface

Jeffrey Tanudji[1], Susan Meñez Aspera[2], Hideaki Kasai[1,2,3]*

[1]*Department of Applied Physics, Graduate School of Engineering, Osaka University, 1-1 Yamadaoka, Suita, Osaka 565-0871, Japan*
[2]*National Institute of Technology, Akashi College, 679-3 Nishioka, Uozumi-cho, Akashi, Hyogo 674-8501, Japan*
[3]*Institute of Radiation Sciences, Osaka University, 1-1 Machikaneyama-cho, Toyonaka, Osaka 560-0043, Japan*

Correspondence
Hideaki Kasai
Department of Applied Physics, Graduate School of Engineering, Osaka University, 1-1 Yamadaoka, Suita, Osaka 565-0871, Japan
E-mail: kasai@dyn.ap.eng.osaka-u.ac.jp

- Received Date: 20 Oct 2022
- Accepted Date: 24 Oct 2022
- Publication Date: 28 Oct 2022

Copyright
© 2022 Authors. This is an open- access article distributed under the terms of the Creative Commons Attribution 4.0 International license.

Abstract

Radioactive iodine (e.g. I-125, I-131) have been used for decades in the medical community for cancer treatment and imaging. Using gold nanoparticles as a carrier for iodine opens possibilities of new treatments for cancer and also for tracking cancerous cells. To design an optimized version of gold nanoparticle for such purpose, we need to understand the bonding mechanism and gauge the strength of such bonding. To this end we performed theoretical calculations on the adsorption state of iodine on gold (111) surface. The results show good adsorption of iodine to gold, most stably on the hollow sites. The bonding mechanism is via the hybridization of the 5p orbital of the iodine with the 6s and 5d orbitals of the neighboring gold atoms. These results act as a first step to designing an optimized gold nanoparticle that can be used in future radiotherapy treatments.

Introduction

Iodine is an important element for the regulation of bodily function, in particular of the thyroid gland [1,2]. Other than I-127, which is stable, the majority of iodine isotopes are radioactive isotopes, such as I-123, I-131, etc. These are commonly used either for imaging purposes or as treatment options against cancerous cells [3]. Since iodine is absorbed by the thyroid gland, the main target for these radioactive iodines are the thyroid cancer cells [4–10]. The prospect of using radioactive iodine to target other types of cancer cells is difficult due to the fact outlined above. In order to expand the use of iodine, another method must be utilized in such a way as to hold the iodine until it reaches the intended target. One possible method is to mount iodine on gold nanoparticles (AuNP).

AuNPs have been studied for use in nanomedicine for various purposes [11–18]. Most uses are utilizing its unique properties of Au itself such as its tunable optoelectronic properties, biocompatibility and non-toxicity in cells among others. In recent years, AuNPs are being developed as a carrier of medicine. In this scenario, AuNPs labeled (or attached) with cancer-fighting drugs can be conjugated with cancer-targeting proteins in order to bind only to certain cancerous cells. Once there, the drugs can be released and therefore would only target the cancerous cells instead of roaming around the body of the patients. This is a great advantage since an optimal amount of drugs for treatment can be used, which minimizes side effects and also keeps the patients from having an excess of medicine in their bodies. In particular for radioactive applications, imaging or tracing agents can also be augmented onto the surface of the nanoparticles, allowing medical personnel to monitor the treatment process without any delay [18]. Additionally, due to the unique properties of Au, external treatments in conjunction with radiotherapy can be applied to the patient should the need arise.

This flexibility allows for the labeling of radioactive iodine on AuNPs, increasing the viability of iodine as a radioactive treatment option for various types of cancer. Not limited to just treating thyroid diseases, these radioactive iodine such as I-125 and I-131 can now be utilized against other types of cancer, provided the proper proteins are conjugated onto the AuNPs [19,20].

Citation: Tanudji J, Aspera SM, Kasai H. Computational Nanomaterials Design: Towards The Realization of Nanoparticle Use in Radiotherapy Case Study 1: Adsorption States of I on Au(111) Surface. Med Clin Sci. 2022; 4(4):19-24.

While experiments have shown that iodine can bond with Au, there are still questions on how well such bonding can hold up. Kim et al. showed cases whereby iodine is found detached from the AuNPs [22]. This could cause potential issues of rouge iodine particles going towards the thyroid, which may be healthy, and cause adverse effects due to the unintended radioactivity in the organ. Several studies have shown that exposure of healthy thyroid cells to radioactive iodine increases the likelihood of thyroid cancer [21,23,24].

Since results from experiments and clinical trials are promising, they can provide the basis for the design of an optimized AuNP that can be used in this purpose. However, as we mentioned before, few articles look at the fundamental science of the nature of bonding behind this adsorption process, such as how iodine bonds with the gold surface [25]. There are interesting insights to be obtained, and can provide us with the understanding needed to design such AuNPs. For this, we have to turn to Computational Materials Design.

The concept of Computational Materials Design (CMD ®) is to find out the fundamental mechanism of the process before designing a methodology to optimize the material for various applications [26]. The use of first principles calculation helps us to virtually design materials with desired characteristics in order to provide the best product that can then be verified by experimentalists before undergoing production. Some examples of CMD ® in application are fuel cells, hydrogen fuel storage, NO catalyst, and investigation of melanin chemistry among others [27–31].

Using CMD ®, we aim to design an optimized AuNP that can be used in radiotherapy. To do this, we need to quantify the strength of adsorption for iodine on AuNP to ensure its stability when it is in operation. Therefore, we first have to understand the physics of adsorption of iodine on AuNP.

Computational details

First principles calculations based on the density functional theory (DFT) were performed using the Vienna ab initio simulation package (VASP) [32,33]. Pseudopotential based on the generalized gradient approximation (GGA) with Perdew, Burke, and Ernzerhof (PBE) exchange-correlation functional was used, along with the projector augmented wave (PAW) method to approximate the core electrons [34–36]. Calculations incorporating van der Waals (vdW) interaction were performed by applying the DFT-D3 method developed by Grimme et al. [37] The electronic one-particle wavefunctions were expanded in a plane-wave basis set up to an energy cut-off of 400 eV, and the convergence criterion for the electronic self-consistency calculation is set at 10^{-5} eV. The integration for the first Brillouin zone is performed using a mesh of 5x5x1 k-points with a Monkhorst-Pack sampling scheme [38].

The calculation model was made using a 3x3 slab of 5 layers of Au(111) separated by a vacuum of 12 Å. The bottom two layers are kept fixed in the bulk configuration while the top three layers are allowed to relax. A schematic of the clean Au(111) surface is shown in figure 1 with possible adsorption sites labeled.

Based on Au bulk calculations, the lattice constant obtained is 4.17 Å for calculations without vdW interaction (non-vdW) and 4.12 Å for calculations involving vdW interaction, which is in range with the value of 4.0786 Å, given in the CRC Handbook of Chemistry and Physics [39]. The adsorption energies for I/Au(111) can be calculated by

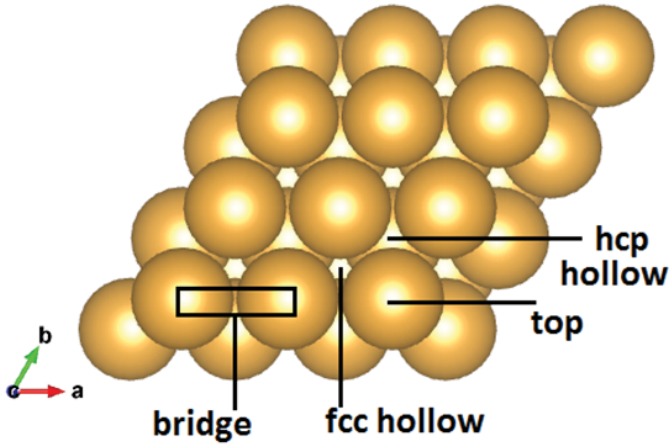

Figure 1. *Adsorption sies of Au(111) surface.*

$$E_{bonding} = E_{I/Au(111)} - \left(0.5 \times E_{I_2} + E_{Au(111)}\right) \quad (1)$$

where $E_{I/Au(111)}$ represents the energy of a single iodine atom adsorbed on the Au(111) slab model, E_{I_2} is the energy of the isolated iodine molecule, and $E_{Au(111)}$ is the energy of the clean Au(111) slab, with or without vdW in the appropriate calculation scheme.

Bader charge calculations using the valence electrons are performed to determine the charge transfers that may happen during the adsorption process [40]. Positive values means an excess of charge (electrons) is present compared to the initial Bader charge calculation for the particular atom. Conversely, a negative value indicates charges going out of the surrounding of the atom.

Results and discussion

This work is going to focus on the interaction between iodine and the surface of an Au slab. While nanoparticle sizes can vary, Kleis et al. found that above a certain threshold, the surface adsorption characteristics of an AuNP approaches that of an Au surface [41]. This approximation allows for representation of bigger nanoparticle sizes which may contain hundreds of atoms as surface slabs and therefore removes additional burden to the computational process. For the choice of surface, we picked the (111) surface as a starting point in our calculation due to it being the most stable among the surfaces [42,43].

The first part of the calculation is obtaining the bonding energy between iodine and the Au surface. Based on the possible adsorption sites, the results of the calculation are shown in table 1.

From the results, we can see that iodine will be more likely to bind on the hollow sites. The negative values show that iodine readily binds to Au surface, with the more negative values indicating a more stable adsorption configuration. We can see a difference of about 0.01 eV between adsorption on fcc hollow and hcp hollow, due to the hollow sites offering three Au atoms for the iodine to attach. The van der Waals (vdW) calculation shows a much bigger effect on the adsorption energy due to the added interactions between the iodine atom and the immediate gold atoms. Both the non-vdW and vdW

Table 1. *Adsorption energies of I on Au(111) surface.*

Position	Adsorption energy (w/o vdW) [eV]	Adsorption energy (w/ vdW) [eV]
bridge	-0.854	-1.285
fcc hollow	-0.916	-1.334
hcp hollow	-0.903	-1.325
top	-0.622	-1.116

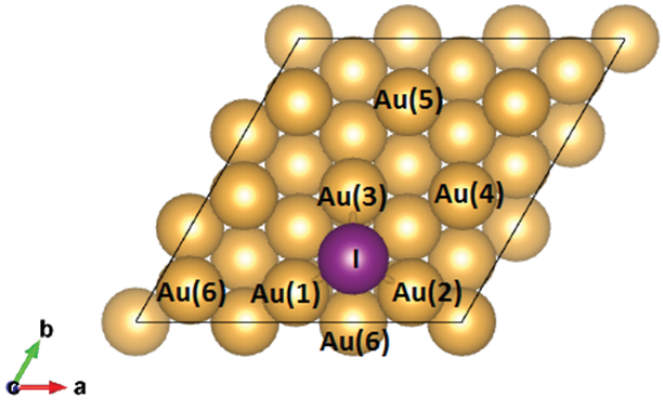

Figure 2. *Schematic diagram of I on Au fcc hollow.*

Table 2.*Bader charges of I on Au(111) surface.*

Atom	Relative charge (before adsorption) [e/atom]	Relative charge (after adsorption) [e/atom]	Difference [e/atom]
I	0	0.0740	0.0740
Au(1)	0.0304	0.0024	-0.0280
Au(2)	0.0304	0.0024	-0.0280
Au(3)	0.0304	0.0099	-0.0205
Au(4)	0.0352	0.0176	-0.0176

calculations show the preference of iodine to hollow sites, with the fcc hollow site showing the most stable adsorption configuration. All electronic calculations are based on the iodine adsorbing on the fcc hollow site (Figure 2).

Next, we look at the charge distribution of the system to understand the bonding between the iodine and the neighboring gold atoms. Bader charge analysis is performed and the result is given in table 2.

We can see that the charge distributions before and after adsorption are not very different from each other. This indicates that electrons are being shared between the incoming iodine and the surrounding Au atoms, creating a covalent bonding. The reason is due to the large work function of Au which allows for a smaller charge transfer to electronegative adsorbates, which causes the bonding to become mostly covalent [44]. Iodine becomes slightly more negative while the Au atoms lose their electrons at a much smaller portion.

Table III provides a comparison between calculations with and without vdW correction.

Based on table III, considering vdW interaction causes a small change in the overall configuration and surface reconstruction of the Au(111). The differences between the two methods are less than 0.1 Å, which is not significant in this system. The height of the iodine atom above the Au surface is obtained to be 2.229 Å and 2.246 Å for the non-vdW and the vdW interaction respectively. This, combined with the overall lack of difference between the distances of the two methods show an overall similarity in the geometry of the adsorption of iodine on Au.

The presence of bonding is visible in the contour plots shown in figure 3 between the iodine atom and the corresponding Au atom, labeled in this case as Au(3). The contour lines have an interval of 0.1 e/Å^3 and the lines closest to the bonding atoms are labeled with numbers to indicate the distribution of charge. It can be seen that between the iodine atom and the Au(3) atom, the charge density falls between the 0.3 and 0.4 e/Å^3 contour lines, whereas between the Au atoms, the charge density is between 0.2 and 0.3 e/Å^3 contour lines. This indicates

Table 3. *Interatomic distances of selected atoms in the I/Au(111) system.*

Atoms	Distance (w/o vdW) [Å]	Distance (w/ vdW) [Å]
I-Au(1)		
I-Au(2)	2.879	2.874
I-Au(3)		
Au(1)-Au(2)		
Au(2)-Au(3)	3.156	3.105
Au(1)-Au(3)		
Au(3)-Au(4)	2.977	2.936
Au(4)-Au(5)	2.942	2.907
Au(1)-Au(6)	3.000	2.969
Au(2)-Au(6)		
Au(1)-Au(7)	2.846	2.818
Bulk Au	2.949	2.913

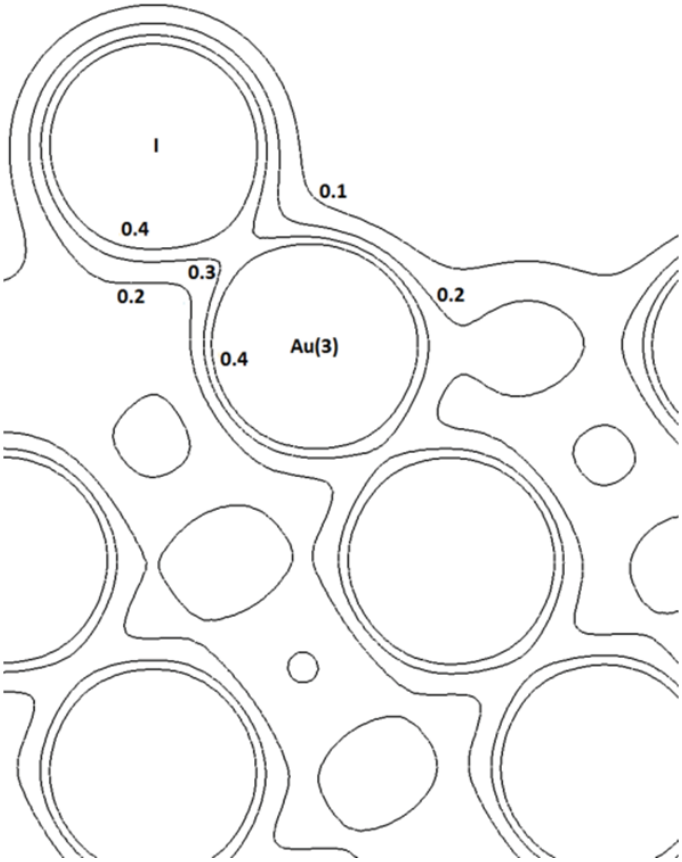

Figure 3. *Charge distribution contour for I/Au(111) taken at the (210) plane, with 0.1 e/Å^3 spacing between the lines.*

that more electrons are being shared between iodine and gold compared to between gold and other gold. While this figure only shows one bonding between the iodine and gold atom, and due to the symmetry of the adsorption position, iodine actually bonds with the three neighboring gold atoms (Au(1), Au(2), and Au(3) of Figure 2) which stabilizes the bonding between the iodine atom and the gold surface.

Finally, we look at the bonding properties through the plots for the density of states (DOS). Figure 4 shows two sets of lines: the dotted lines represent the DOS of the gold valence orbitals before adsorption (clean) and the full lines represent the DOS of the gold valence orbitals after adsorption (bond). The purple line represents the I 5p orbital after it has been adsorbed on the surface. We can see the energy range of I 5p orbital falls along the same energy ranges of Au 6s and Au 5d

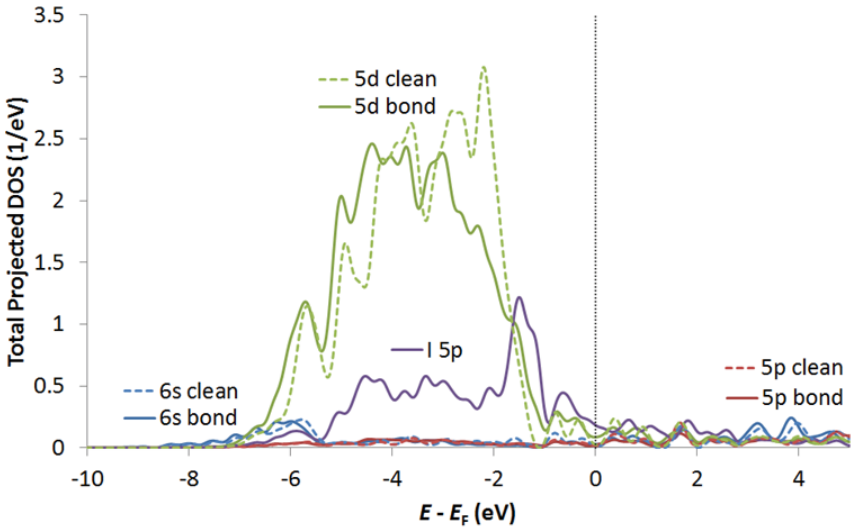

Figure 4. *Projected DOS of I/Au(111) system.*

orbitals. The hybridization between Au 6s and I 5p, as well as the hybridization between the Au 5d and the I 5p can be seen from the shape of the I 5p, which tends to follow both gold orbitals along the I 5p orbital energy range.

A comparison of the "clean" and "bond" lines gives the effect due to the bonding, especially in the hybridization of the DOS of gold. It can be seen that prior to the adsorption process, the Au 5d has slightly more states near the Fermi level, but after the adsorption, more states appear in the lower energy regime of the Au 5d, indicating a more stable configuration. Additionally, the DOS of the Au 5d orbital has been slightly broadened, particularly near the Fermi energy. This indicates that some electrons were transferred from the 5d orbital to some other orbitals such that the orbital is able to take part in the adsorption process.

One aspect of covalent bonding is the hybridization of the affected orbitals, and that is seen in the Au 5d orbital with the I 5p. Several energy levels, especially from -4.5 eV to -2 eV, show the Au 5d DOS following the shape of the I 5p DOS, modifying the original DOS of the Au 5d. This strengthens our belief that the I bonds with Au covalently, which is in agreement with the experimental result [25].

Another orbital affected by this adsorption process is the Au 6s, which can be seen around -6 eV and near the Fermi level. However, since the changes are relatively small, we think the adsorption process is driven mainly by the hybridization of the I 5p and Au 5d orbitals with some contribution from the I 5p and Au 6s orbital hybridization.

The purpose of this study is to learn the basic mechanism by which iodine can be attached to AuNPs, and also act as an initial starting point to more complex studies which make the design process more feasible. Therefore, we are looking at the most basic case of pure iodine and pure gold, without any external factors. We hope to start exploring the various possibilities of iodine adsorption on Au, which can provide us with both quantitative information and also about the qualitative trends and possible problems that can arise from this treatment methodology.

Conclusion

In this work, we have calculated the adsorption state of iodine on Au(111) surface in order to understand the nature of the bonding between the radioactive substance and its carrier. Experiments have shown that iodine can bond strongly with AuNPs. Based on our calculations, it seems that iodine can indeed bond with Au surface. The primary mechanism for bonding is the hybridization of the I 5p orbital with the surrounding Au atoms' 6s and 5d orbitals, which allows for the continued attachment of iodine on Au.

This result serves as a starting point and benchmark for future works, with the eventual goal of designing an optimal nanoparticle for use in this field. Considering the history and many potential uses of iodine, this work hopes to advance our understanding of the use of such treatments to help patients cope with their illness and hopefully make a full recovery.

Acknowledgement

Calculations were performed in Nakanishi laboratory at NIT, Akashi College, as well as the Yukawa Institute for Theoretical Physics (YITP) at Kyoto University. The authors appreciate the discussions with Prof. Wilson A. Diño, Prof. Michio Okada, and Prof. Tetsuo Ogawa. JT is thankful for the financial support provided by both the Matsuda Yosahichi Memorial Foundation for Foreign Students as well as Osaka University.

References

1. Food and Agriculture Organization of the United Nations and the World Health Organization, Human Vitamin and Mineral Requirements: Report of a joint FAO/WHO expert consultation, Bangkok, Thailand (FAO Rome, Rome, Italy, 2001) chpt. 12, p. 181.
2. Zimmermann MB. Iodine deficiency. Endocr Rev. 2009;30(4):376-408.
3. Schlyer DJ. Production of radioactive iodine (International Atomic Energy Agency, 2002), p. 103.
4. Werner SC, Quimby EH, Schmidt C. Radioactive iodine, I-131,

in the treatment of hyperthyroidism. Am J Med. 1949;7(6):731-740.

5. Beierwaltes WH. The history of the use of radioactive iodine. Semin Nucl Med. 1979;9(3):151-155.
6. Hertz S, Roberts A. Radioactive iodine in the study of thyroid physiology; the use of radioactive iodine therapy in hyperthyroidism. J Am Med Assoc. 1946;131:81-86.
7. Stokkel MP, Handkiewicz Junak D, Lassmann M, Dietlein M, Luster M. EANM procedure guidelines for therapy of benign thyroid disease. Eur J Nucl Med Mol Imaging. 2010;37(11):2218-2228.
8. Silberstein EB, Alavi A, Balon HR, et al. The SNMMI practice guideline for therapy of thyroid disease with 131I 3.0. J Nucl Med. 2012;53(10):1633-1651.
9. Wei S, Li C, Li M, et al. Radioactive Iodine-125 in Tumor Therapy: Advances and Future Directions. Front Oncol. 2021;11:717180.
10. Mettler, Jr. FA, Guiberteau MJ. Essential of Nuclear Medicine and Molecular Imaging. 7th Edtn. Elsevier, Philadelphia, 2019. p. 86.
11. Au JT, Craig G, Longo V, et al. Gold nanoparticles provide bright long-lasting vascular contrast for CT imaging. AJR Am J Roentgenol. 2013;200(6):1347-1351.
12. El Ketara S, Ford NL. Time-course study of a gold nanoparticle contrast agent for cardiac-gated micro-CT imaging in mice. Biomed Phys Eng Express. 2020;6(3):035025.
13. Boisselier E, Astruc D. Gold nanoparticles in nanomedicine: preparations, imaging, diagnostics, therapies and toxicity. Chem Soc Rev. 2009;38(6):1759-1782.
14. Hu M, Chen J, Li ZY, et al. Gold nanostructures: engineering their plasmonic properties for biomedical applications. Chem Soc Rev. 2006;35(11):1084-1094.
15. Kim S-H, Kim E-M, Lee C-M, et al. Synthesis of PEG-Iodine-Capped Gold Nanoparticles and Their Contrast Enhancement in In Vitro and In Vivo for X-Ray/CT. Journal of Nanomaterials. 2012;504026.
16. Yeh YC, Creran B, Rotello VM. Gold nanoparticles: preparation, properties, and applications in bionanotechnology. Nanoscale. 2012;4(6):1871-1880.
17. Silva F, Paulo A, Pallier A, et al. Dual Imaging Gold Nanoplatforms for Targeted Radiotheranostics. Materials (Basel). 2020;13(3):513.
18. Daems N, Michiels C, Lucas S, Baatout S, Aerts A. Gold nanoparticles meet medical radionuclides. Nucl Med Biol. 2021;100-101:61-90.
19. Sun N, Zhao L, Zhu J, et al. 131I-labeled polyethylenimine-entrapped gold nanoparticles for targeted tumor SPECT/CT imaging and radionuclide therapy. Int J Nanomedicine. 2019;14:4367-4381.
20. Li Q, Tian Y, Yang D, Liang Y, Cheng X, Gai B. Permanent Iodine-125 Seed Implantation for the Treatment of Nonresectable Retroperitoneal Malignant Tumors. Technol Cancer Res Treat. 2019;18:1533033819825845.
21. Robbins J, Schneider AB. Thyroid cancer following exposure to radioactive iodine. Rev Endocr Metab Disord. 2000;1(3):197-203.
22. Kim YH, Jeon J, Hong SH, et al. Tumor targeting and imaging using cyclic RGD-PEGylated gold nanoparticle probes with directly conjugated iodine-125. Small. 2011;7(14):2052-2060.
23. Holm LE. Thyroid cancer after exposure to radioactive 131I. Acta Oncol. 2006;45(8):1037-1040.
24. Ron E. Thyroid cancer incidence among people living in areas contaminated by radiation from the Chernobyl accident. Health Phys. 2007;93(5):502-511.
25. Walsh AA. Chemisorption of iodine-125 to gold nanoparticles allows for real-time quantitation and potential use in nanomedicine. J Nanopart Res. 2017;19(4):152.
26. Kasai H, Akai H, Yoshida H. Computational Materials Design from Basics to Actual Applications. Chapter 2. Osaka University Press, Suita, Japan. 2005. (in Japanese)
27. Kasai H, Tsuda M. Computational Materials Design, Case Study I: Intelligent/Directed Materials Design for Polymer Electrolyte Fuel Cells and Hydrogen Storage Applications. Osaka University Press, Suita, Japan. 2008. (in Japanese)
28. Kasai H, Escaño MCS. Physics of Surface, Interface and Cluster Catalysis. IOP Publishing, Bristol, UK. 2016.
29. Kasai H, Padama AAB, Chantaramolee B, Arevalo RL. Hydrogen and Hydrogen-Containing Molecules on Metal Surfaces. Springer, Singapore, 2020.
30. Aspera SM, Arevalo RL, Chantaramolee B, Nakanishi H, Kasai H. PdRuIr ternary alloy as an effective NO reduction catalyst: insights from first-principles calculation. Phys Chem Chem Phys. 2021;23(12):7153-7163.
31. Kishida R, Aspera SM, Kasai H. Melanin Chemistry Explored by Quantum Mechanics. Springer, Singapore, 2021.
32. Kresse G, Furthmüller J. Efficient iterative schemes for ab initio total-energy calculations using a plane-wave basis set. Phys Rev B Condens Matter. 1996;54(16):11169-11186.
33. Kresse G, Furthmüller J. Efficiency of ab-initio total energy calculations for metals and semiconductors using a plane-wave basis set. Comput Mater Sci. 199;6:15.
34. Perdew JP, Burke K, Ernzerhof M. Generalized Gradient Approximation Made Simple. Phys Rev Lett. 1996;77(18):3865-3868.
35. Blöchl PE. Projector augmented-wave method. Phys Rev B Condens Matter. 1994;50(24):17953-17979.
36. Kresse G, Joubert D. From ultrasoft pseudopotentials to the projector augmented-wave method. Phys Rev B: Condens Matter Mater Phys. 1999;59:1759.
37. Grimme S, Ehrlich S, Goerigk L. Effect of the damping function in dispersion corrected density functional theory. J Comput Chem. 2011;32(7):1456-1465.
38. Monkhorst HJ, Pack JD. Special points for Brillouin-zone integrations. Phys Rev B: Condens. Matter Mater Phys. 1976;13:12.
39. Lide DR, Ed., CRC Handbook of Chemistry and Physics. (86th edtn)Taylor & Francis Group, Florida, 2005. p. 4-150.
40. Henkelman G, Arnaldson A, Jónsson H. A fast and robust algorithm for Bader decomposition of charge density. Comput Mater Sci. 200;36:254.
41. Kleis J, Greeley J, Romero NA, et al. Finite Size Effects in Chemical Bonding: From Small Clusters to Solids. Catal Lett. 2011;141:1067.
42. Grochola G, Snook IK, Russo SP. On fitting a gold embedded atom method potential using the force matching method. J Chem Phys. 2007;127:224704.
43. Holec D, Dumitraschkewitz P, Vollath D, Fischer FD. Surface Energy of Au Nanoparticles Depending on Their Size and Shape. Nanomaterials (Basel). 2020;10(3):484.
44. Roman T, Gossenberger F, Forster-Tonigold K, Groß A. Halide adsorption on close-packed metal electrodes. Phys Chem Chem Phys. 2013;16:13630.